

GIS methodology and case study regarding assessment of the solar potential at territorial level: PV or thermal?

Loïc Quiquerez*, Jérôme Faessler, Bernard Lachal, Floriane Mermoud and Pierre Hollmuller

Institute Forel & Institute for Environmental Sciences, University of Geneva, route de Drize 7, 1227 Carouge, Switzerland

ABSTRACT

This paper presents a GIS-based methodology for assessing solar photovoltaic (PV) and solar thermal potentials in urban environment. The consideration of spatial and temporal dimensions of energy resource and demand allows, for two different territories of the Geneva region, to determine the suitable building roof areas for solar installations, the solar irradiance on these areas and, finally, the electrical and/or thermal energy potentials related to the demand. Results show that the choice of combining PV and solar thermal for domestic hot water (DHW) is relevant in both territories. Actually, the installation of properly sized solar thermal collectors doesn't decrease much the solar PV potential, while allowing significant thermal production. However, solar collectors for combined DHW and space heating (SH) require a much larger surface and, therefore, have a more important influence on the PV potential.

Keywords:

Solar energy;
Photovoltaic;
Solar thermal;
Solar mapping;
Energy planning
URL:
dx.doi.org/10.5278/ijsepm.2015.6.2

1. Introduction

The depletion of fossil resources and the environmental impacts of energy production require reconsidering the energy systems. In this context, solar energy is particularly interesting because the resource is inexhaustible, well distributed and its exploitation has few impacts regarding GHG-emissions. In urban environment characterized by a strong land use, decentralized solar energy production - defined as solar installations on the roofs of buildings as opposed to large scale solar plants - appears as one of the most adequate solutions, but its potentials are still poorly defined at the scale of a city. Today policy makers and other actors involved in the development of solar energy need tools to quantify these potentials and to assess the spatial competition between photovoltaic and solar thermal energy.

Several studies based on different approaches have developed models to assess solar resource at various scales: world [1], continent and nation [2, 3], region

[4, 5], city and district [6-11]. An increasing number of solar mapping tools are arising, with different data type, resolution, calculation methods and mapping outputs [12]. These studies are mostly focalized on solar resource and PV potential assessment, but hardly on solar thermal potential, even if there are some researches taking place in this field [13,14]. In most cases, solar thermal potential is evaluated from extrapolations based on samples, without being coupled with GIS [15].

This study deals with two main ways of producing decentralized useful energy from solar resource on the roofs of a given territory: the first one by way of photovoltaic production (scenario 1) and the second one through solar thermal production for DHW only (scenario 2) or for combined DHW and SH (scenario 3). In scenarios with solar thermal production (2 and 3), complementary PV on possible spare suitable roof areas is added in order to analyze the spatial competition between solar thermal and PV. The method developed was tested

* Corresponding author - e-mail : loic.quiquerez@unige.ch

Nomenclature and subscripts

<i>E</i>	Photovoltaic production (kWh/m ² /day)
<i>G</i>	Global solar irradiation on solar installation (kWh/m ² /day)
<i>Q</i>	Solar heat production (kWh/m ² /day)
<i>Q₀</i>	Solar thermal effective heat loss (kWh/m ² /day)
<i>S</i>	Specific collector area (m ² /pers)
<i>η</i>	Effective system efficiency (-)
<i>ΔT</i>	Temperature differential between delivered heat and outdoor (K)
<i>GIS</i>	Geographic information system
<i>DHW</i>	Domestic hot water
<i>PV</i>	Photovoltaic
<i>SH</i>	Space heating

and analyzed for two different territories of Geneva in Switzerland (city center and rural suburban town).

2. Methodology

2.1. Input data and general methodology

Table 1 presents the required spatial and meteorological data used in the model to estimate the PV and solar thermal potentials for two territories in Geneva, Switzerland. Spatial data are derived from the land information system of the State of Geneva [16] and meteorological data from the Energy Group of the University of Geneva [17]. Figure 1 presents the general methodology for the elaboration of the three scenarios: 100% PV (sc.1), solar thermal for DHW with

complementary PV (sc.2), and solar thermal for SH and DHW with complementary PV (sc. 3). It should be noticed that data related to the population and the total heat consumption per buildings are necessary in order to assess the solar thermal potential which is closely linked to the demand. As the total heat consumptions in buildings are not available for one of the two territories studied, the third scenario is performed for only one of them.

2.2. Solar resource mapping

Solar resource mapping is elaborated using the solar analyst tool “solar radiation” developed by Fu and Rich [18] and integrated in the GIS software ArcGIS [19]. This model based on solar geometrical theory derives

Table 1: Input data.

	Source	Object	Acquisition	Accuracy	Type
GIS data	Land information system of the state of Geneva	Digital Surface Model (DSM)	LIDAR (Light Detection And Ranging)	Grid-cell 1m × 1m Vertical accuracy: 0.15 m Planimetric accuracy: 0.5 m	Raster
		Population by address	Census		Point
	Buildings, roofs and superstructures	Annual buildings heat consumption	Photogrammetry	Vertical accuracy: 0.3 m Planimetric accuracy: 0.3 m	Polygon
			Meter reading		Polygon
Meteorological data	Energy Group, University of Geneva	Global irradiance on horizontal plane (Gh)	Monitoring: Kipp & Zonen CM10	~2%, calibrated each year against a sub-standard	Ground measurements
		Normal beam irradiance (Bn)	Monitoring: Eppley NIP	~2%, calibrated each year against an absolute cavity radiometer	Ground measurements
		Diffuse irradiance on horizontal plane (Dh)	Calculation: Dh = Gh-Bn·sin (h)		
		External temperature	Monitoring : PT100	± 0.1 °C	Ground measurements

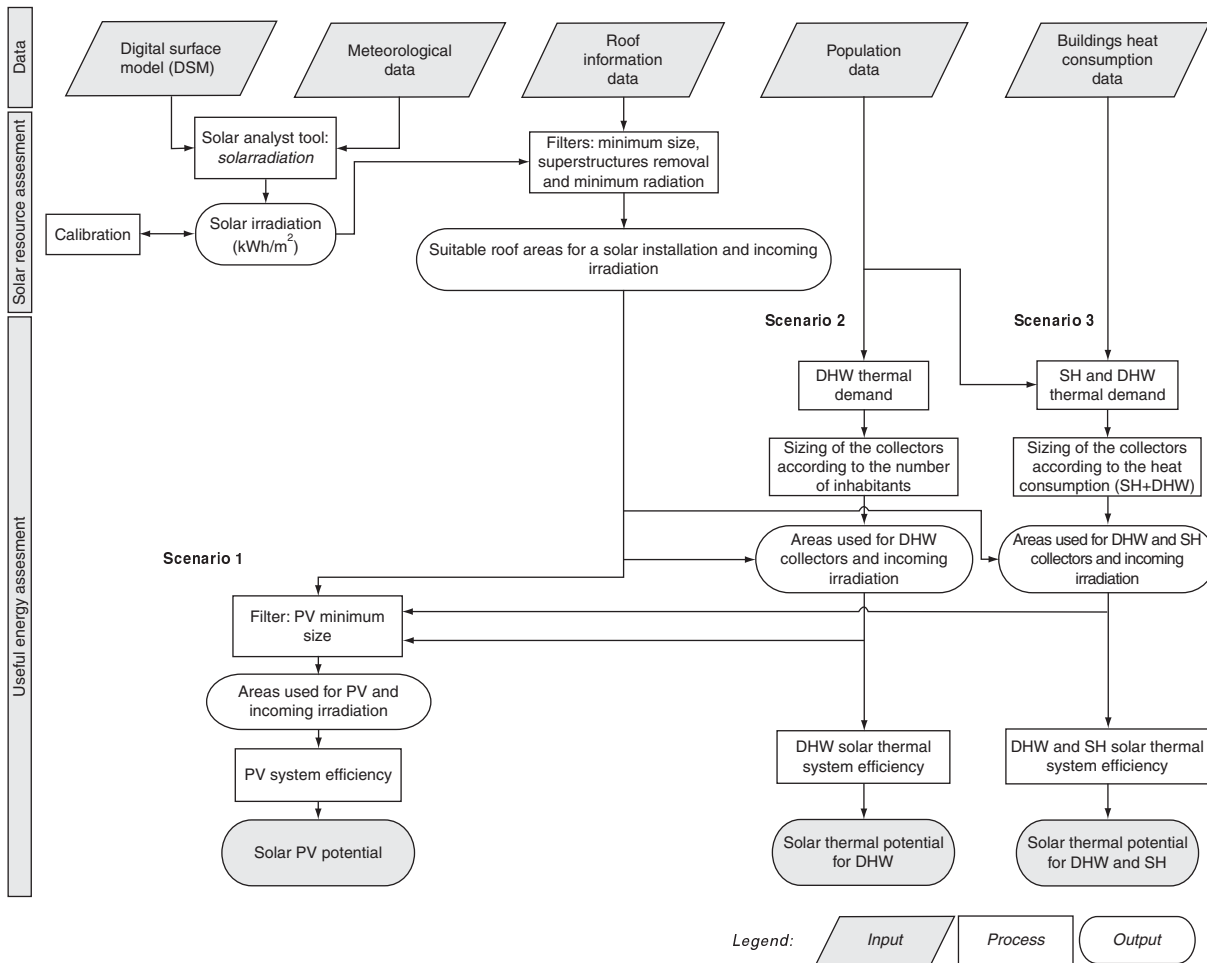


Figure 1: General methodology.

incoming solar irradiation for each pixel of a Digital Surface Model (DSM) which characterizes the topography of the area (elevation, slope and orientation). Several input parameters are required such as latitude, atmospheric transmittance and proportion of diffuse to global solar irradiation. The calculation process for each pixel is based on a viewshed map generation coupled with a sunmap and a skymap in the same upward-looking hemispherical projection [19]. The sunmap is a raster that displays the sun track into a series of sectors as the sun varies through the hours of the day and the day of the year, and from which beam irradiation is calculated. The skymap displays the entire sky divided into multiple sectors, and from which diffuse irradiation is calculated. Sectors are defined by 16 azimuth and 8 zenith angles depending on the time and the location.

For assessment of the seasonal dynamic, the daily global solar irradiation is calculated for a typical day of

each month, on each pixel, in a half hour time step. Generally in the middle of the month, this day represents the monthly average solar geometry characteristics. A calibration process (adjustment of the atmospheric transmittance) ensures that the sum of direct and diffuse solar irradiation on a horizontal plane matches the monthly average value over the 2003-2009 period as monitored at the meteorological station of the University of Geneva (Figure 2), located in the city center. The average measured global horizontal irradiation is 1,297 kWh/m²/yr with a proportion of diffuse to global about 43% [17].

To determine the suitable roof areas for solar production in each building, the solar resource map is intersected with a geographical layer representing the building roof footprints obtained by photogrammetry (from aerial photos), from which were removed roof superstructures (chimneys, etc.) and borders (buffer

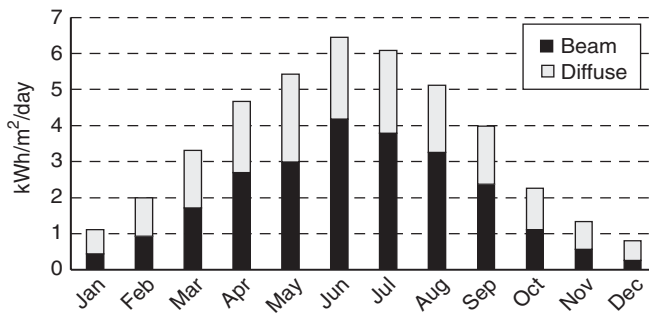


Figure 2: Global horizontal, beam and diffuse irradiation in Geneva, average 2003–2009.

zone of 0.5m). Two filters are applied to take into account economic and technical aspects, in the same way as other studies [20,21]. The first one consists in selecting only pixels with more than 1,100 kWh/m² (and thus taking into account orientation and slope), which is a threshold slightly more conservative than the 1,000 kWh/m² proposed by [22,23]. At this stage of the procedure, raster data (pixels) are converted into vector data (polygons). As the slope of each roof is known, the actual roof areas can be estimated. The second filter consists in selecting only areas larger than 10 m² for elimination of small isolated polygons.

The result of this process is a layer with the suitable roof areas for solar installations and the amount of global solar irradiation on these areas. In a next step (section 2.3), we will further apply appropriate sizing rules for determination of the actual roof area to be used, according to the type of valorization considered (PV, DHW, SH).

2.3. Useful energy potentials

Transformation of the solar irradiation into useful energy (electricity or heat) is estimated for following three scenarios.

2.3.1. Scenario 1: 100% PV

In this scenario, it is assumed that PV production is fed into the grid and not limited by demand, so that all suitable roof area defined above could in principle be used for this purpose. However, PV installations smaller than 15 m² are usually regarded as economically unprofitable [24], so that suitable areas below this limit are discarded.

PV production E_{PV} is estimated on each area available for PV and for each of the twelve typical days, by way of a constant system efficiency η_{PV} set at 12% [7]:

$$E_{PV} = \eta_{PV} \cdot G \quad (1)$$

The monthly and annual production potentials are straightforwardly extrapolated taking into account the number of days of each month.

2.3.2. Scenario 2: solar thermal for DHW production, with complementary PV

Unlike PV production, solar thermal for DHW production is influenced by the sizing related to the building DHW demand, i.e. to the number of inhabitants.

For each building, DHW demand is estimated thanks to the number of inhabitants and a typical average daily consumption of 50 liters per person at 55°C (2.45 kWh/pers/day), with a slight seasonal variation due to occupancy rate and cold water temperature level (maximum of 2.98 kWh/pers/day in January, minimum of 1.51 kWh/pers/day in July), as observed on typical residential buildings in Geneva [25].

The sizing rule for the DHW solar collectors which is used in this study is inspired by the Swiss sizing guide for solar thermal collectors [26] and corresponds to technically and economically acceptable solutions [27]. It is given in terms of a demand specific collector area of 0.7 m²/pers for large multifamily buildings, which increases in the case of few consumers (Table 2), taking into account the size independent costs. For each building, the effective thermal collector area is determined by preceding sizing rule, which is then compared to the suitable roof area to ensure that there is enough space for it. In case of missing area, the sizing is reduced until a minimal value fixed at 50% of the initial sizing value. On the contrary, in case of spare suitable roof area, latter is assigned to complementary PV production.

As a next step, the solar production is evaluated for each building and for each of the twelve typical days, by way of a solar thermal input/output diagram which relates the monthly average daily specific solar

Table 2: Sizing rule used to determine the DHW solar thermal collector area. Note: Interpolation of specific collector area between 2 and 20, and 20 and 100 persons.

Number of inhabitants	Specific collector area (m ² /pers)
0 or 1	0
2	1.5
20	1
100 or more	0.7

production Q_{DHW} to the monthly average daily solar irradiation on the collectors G , taking into account the specific collector area S (Figure 3, left).

Such curves were initially developed and validated for daily values, on the basis of physical considerations and models [28,29]. In a second step [30], they were extended to monthly values (average daily values), by the way of numerical simulation on diverse configurations varying size, slope and orientation. The simulated system contains a solar storage tank of 30l/m² for management of the day/night time lag between production and demand, which was set at 2.45 kWh/pers/day.

The correlation between solar irradiation and production is linear [30]:

$$Q_{DHW} = \eta_{DHW} \cdot G - Q_{0_DHW} \quad (2)$$

The effective linear efficiency η_{DHW} and the effective heat loss terms Q_{0_DHW} (taking into account capacitive effects), which depend on the specific collector area, can be approximated by way of following expressions (valid for $0.5 \leq S \leq 2\text{m}^2/\text{pers}$):

$$\eta_{DHW} = 1.035 - 0.764 \cdot S + 0.184 \cdot S^2 \quad (3a)$$

$$Q_{0_DHW} = 0.786 - 1.03 \cdot S + 0.305 \cdot S^2 \quad (3b)$$

Finally, for each typical day of each month and for each building, the solar production (model output) is compared to the actual demand for DHW and excess production is discarded.

The ultimate step is to evaluate the complementary PV production on spare suitable roof area in the same way as for scenario 1.

2.3.3. Scenario 3: solar thermal for combined SH and DHW production, with complementary PV

Solar thermal for combined SH and DHW production has to take into account proper sizing related to the buildings heat demand.

The demand is estimated thanks to the regional geodatabase [16] which, for each building of more than 3 flats, contains the actual demand of final energy (gas or oil) for thermal demand, as averaged and climatically corrected over three recent years. In this study, an average 80% conversion efficiency is considered to estimate the thermal demand (SH + DHW), as it is recommended by Swiss norms edited by the Swiss society of engineers and architects [31]. As for scenario 2, the DHW share of this demand is evaluated through the number of inhabitants, the rest being attributed to SH. Latter is distributed over the year using the monthly heating degree days, finally yielding monthly values of combined SH and DHW demand.

As for DHW, the sizing rule for solar collectors which is used in this study is inspired by the Swiss sizing guide for solar thermal collectors [26]. It is set at a specific value of 0.75 m² collector area per MWh of annual heat demand. The effective thermal collector area is determined by comparing the preceding rule with the suitable roof area. In case of missing area, the sizing is reduced until a minimal value fixed at 50% of the initial sizing value.

The monthly average temperature level of SH demand is evaluated by way of a typical linear heating curve (water heating supply temperature of 55 °C at -8 °C outdoor, and 39 °C at 15 °C outdoor), corresponding

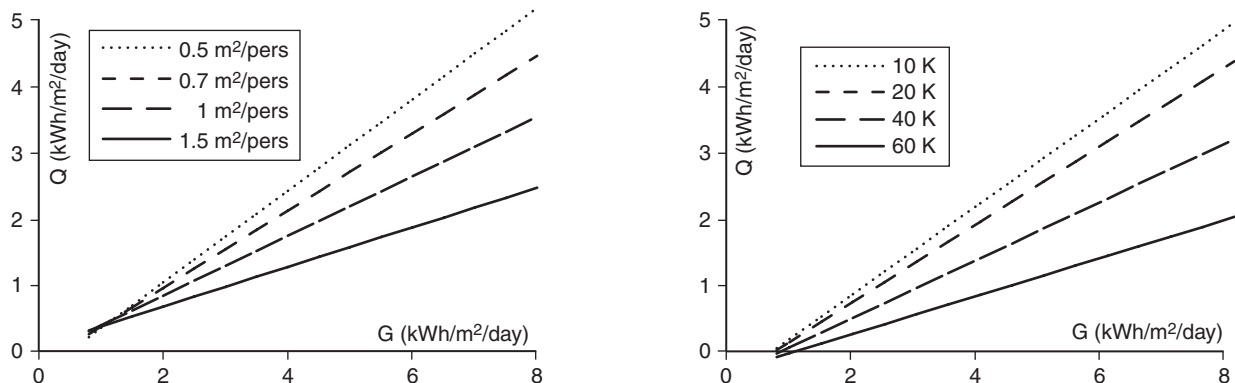


Figure 3: Input/output diagrams for glazed solar thermal collectors, monthly values (average daily values). Left: solar heat production for domestic hot water, for different values of the specific collector area. Right: solar heat production for combined space heating and domestic hot water, for different values of the temperature differential between delivered heat and outdoor.

to the values observed on a sample of 70 multifamily residential buildings in Geneva [32].

In the same way as for the scenario 2, the solar production is evaluated for each building and for each of the twelve typical days, using a solar thermal input/output diagram which relates the monthly average daily specific solar production Q_{SH+DHW} to the monthly average daily solar irradiation on the collectors G , taking into account the temperature differential between delivered heat and outdoor (Figure 3, right). The diagram is a result of numerical simulation on a variety of configurations concerning temperature level for SH, slope and orientation [30]. The model concerns the simplified case of solar collectors directly coupled to the heat distribution circuit (by way of a heat exchanger), with a given temperature level and an infinite load. Such a simplification implies that the day/night time lag between solar irradiation and heat demand has to be managed by an appropriate storage, which is not explicitly taken into account in the simulation.

The correlation between solar irradiation and production is linear [30]:

$$Q_{SH+DHW} = \eta_{SH+DHW} \cdot G - Q_{0_SH+DHW} \quad (4)$$

The effective linear efficiency η_{SH+DHW} and the effective heat loss terms Q_{0_SH+DHW} , which depend on the temperature differential between delivered heat and outdoor, can be approximated by the following expressions (valid for a delivery temperature between 30 and 60 °C):

$$\eta_{SH+DHW} = 0.7523 - 0.0077 \cdot \Delta T \quad (5a)$$

$$Q_{0_SH+DHW} = 0.5347 - 0.0035 \cdot \Delta T \quad (5b)$$

Finally, for each month and building, the solar production (model output) is compared to the actual demand for SH and DHW. Since seasonal storage is not considered, corresponding excess production is discarded. From a technical point of view this implies an appropriate dissipation device, in particular for the summer period.

As before, complementary PV production on spare suitable roof area is finally evaluated in the same way as for scenario 1.

3. Selected territories

This study focuses on two territories of Geneva which have different morphological characteristics (Figure 4

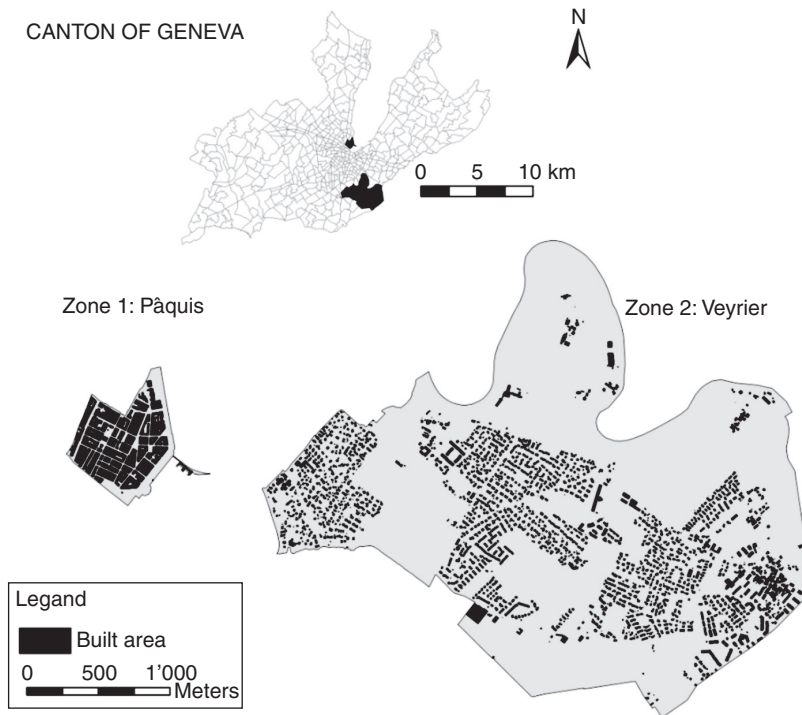


Figure 4: Presentation of the two areas.

and Table 3). The first one represents a dense district of the city center (Pâquis); the second one a rural suburban town (Veyrier). Both territories have about ten thousand inhabitants and were selected from the official territorial division [16]. Some important differences are the built area and its density, and the population density related to the land area and to the built area (see Table 3, right).

4. Results

4.1. Solar resource mapping

In this work, solar resource is considered as the combination of both solar irradiation and available area to capture this irradiation. The results show that the suitable roof areas for solar installations represent 56,244 and 132,313 m², in Pâquis and Veyrier respectively, which corresponds to 25 and 27% of total roof areas and to 5.3 and 14.1 m² per inhabitant (Table 3). A sensitivity analysis shows that a limit fixed at 1,000 kWh/m² for the first filter implies an increase of the suitable roof areas by 6-7%. For the second filter, if the minimal surface is lowered from 10 to 5 m², an increase by 1–2% is observed.

Global solar irradiation on these areas represents 62 and 149 GWh/year. Figure 5 shows an example of the resource map of a portion of Veyrier where the effect of slope, orientation and obstruction (left) can be seen, as well as resulting selected suitable roof footprint areas (right) according to the filters presented in section 2.2. As expected, suitable roof areas are mainly south-facing.

4.2. Useful energy potentials

As an illustration of the above developed GIS methodology and of related results, the following three maps (Figure 6) show, for a portion of Veyrier, the PV potential and the solar thermal potential for scenarios 1 and 2. One can notice that the PV potential is directly related to the size of the building while the solar thermal is not. This is due to the strong interaction between resource and demand for solar thermal application. The bigger building at the top of the map represents a sports center with an important PV potential. Its solar thermal potential is considered as zero because there are no inhabitants. This case illustrates some limitations of the model, thermal needs for domestic hot water actually occurring throughout the year in sports centers.

Table 4 summarizes the entire solar useful energy potentials for both territories according to the three scenarios: 100% PV (sc.1), solar thermal for DHW with complementary PV (sc.2), and solar thermal for SH and DHW with complementary PV (sc. 3).

In the first scenario, the PV potential for both territories is mainly determined by the built area. In Pâquis, it is estimated to be 7,440 MWh against 17,548 MWh in Veyrier. If the average PV productivity is relatively similar, respectively 132 and 136 kWh/m², the production per inhabitant is quite different (699 kWh/pers and 1,865 kWh/pers), due to the population density related to the built area.

Table 3: Morphological and solar resource indicators for both territories

	Pâquis	Veyrier	Ratio Pâquis/Veyrier
Morphological indicators			
Land area (m ²)	412,952	6,496,793	0.1
Built area (m ²)	191,331	467,743	0.4
Built density (m ² /m ²)	0.46	0.07	6.6
Buildings	637	4,052	0.2
Roof area (m ²)	211,897	521,548	0.4
Average slope of the roofs (°)	15.5	21.1	
Population (pers)	10,642	9,411	1.1
Population density (pers/1000m ²)	25.8	1.5	17.2
Population density related to the built area (pers/m ²)	0.06	0.02	3.0
Solar resource indicators			
Suitable roof areas for solar installations (m ²)	56,244	132,313	0.4
Suitable roof areas for solar installations per capita (m ² /pers)	5.3	14.1	0.4
Solar irradiation on suitable roof areas (GWh)	62	149	0.4

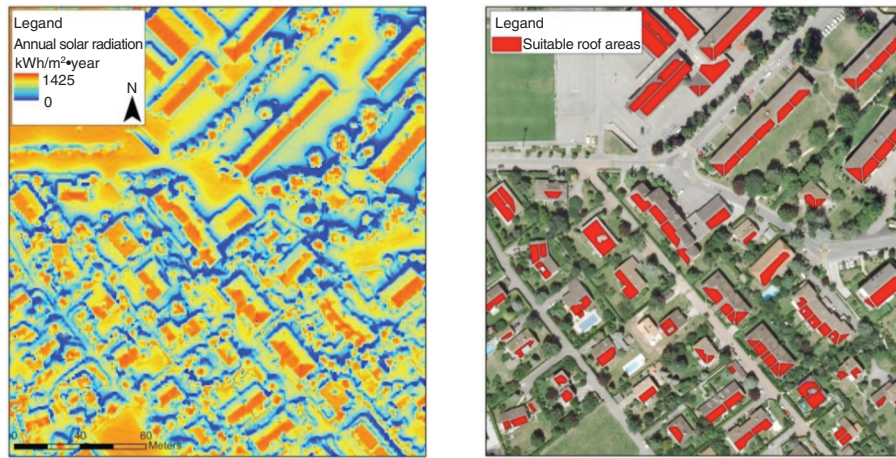


Figure 5: Solar resource mapping (left) and suitable roof areas (right)

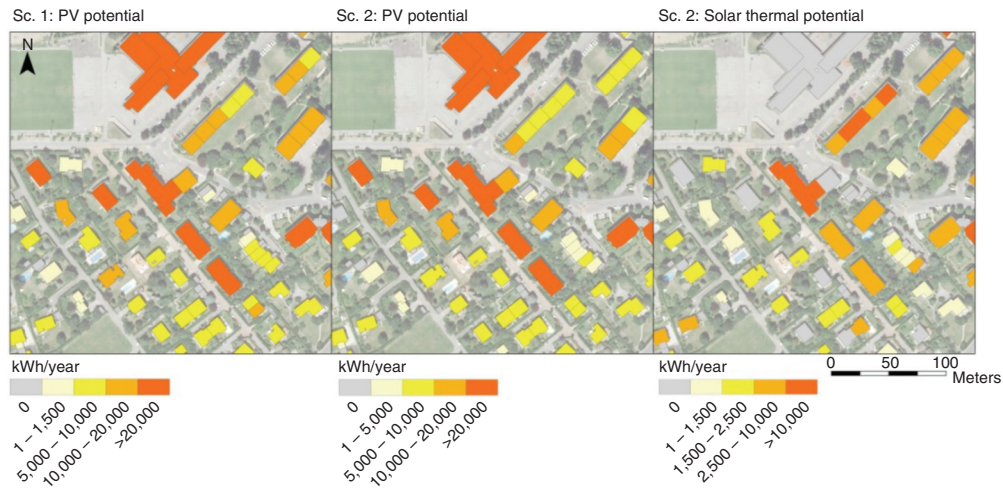


Figure 6: PV potential (in the first and second scenario) and DHW solar thermal potential (second scenario)

Table 4: Useful energy potentials indicators.

Solar useful energy potentials indicators	Scenario 1 PV		Scenario 2 DHW+PV		Scenario 3 SH+DHW+PV
	Pâquis	Veyrier	Pâquis	Veyrier	Pâquis
Roof areas for PV (m ²)	56,165	129,397	46,315	117,549	14,829
PV production (MWh)	7,440	17,548	6,135	15,946	1,947
PV production per pers. (kWh/pers)	699	1,865	576	1,694	183
PV productivity (kWh /m ²)	132	136	132	136	131
Roof areas for solar thermal (m ²)	–	–	9,715	10,969	41,126
Solar thermal production (MWh)	–	–	4,720	4,138	11,525

A monthly analysis shows the PV potential variability throughout the year, with a ratio 7/1 between the month that has the higher solar irradiation and the

lowest one (Figure 7). As the PV system efficiency is assumed constant through the year, this ratio is similar to the one related to the solar resource assessment.

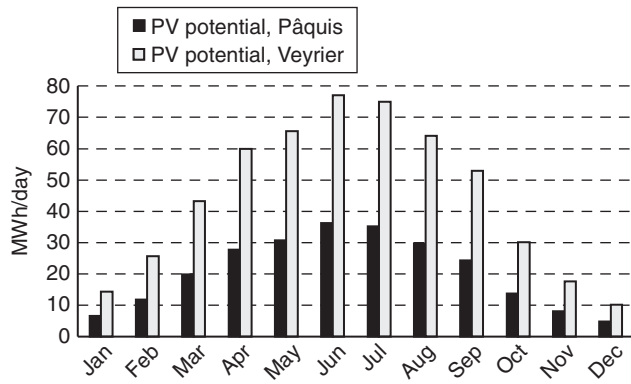


Figure 7: Monthly PV potential in scenario 1.

In the second scenario, the solar thermal potential for DHW in Pâquis is estimated to 4,720 MWh per year for a total collector area of 9,715 m², while in Veyrier it is 4,138 MWh for an area of 10,969 m². The nonlinear relation between collector area and solar production relates to the thermal demand for DHW and the sizing of thermal collectors. In Veyrier, 88% of the roofs on which solar collectors are installed have a collector area between 3 and 9 m², due to a large number of single-family houses with few inhabitants. For them, the sizing of solar collectors is more generous (average of 1.17 m²/pers against 0.91 m²/pers in Pâquis), which implies a decline in productivity. The average productivity is 486 kWh/m² in Pâquis against 377 kWh/m² in Veyrier.

The filter that set the minimal suitable roof area at 10 m² doesn't reduce much the potential for small solar thermal installations (less than 10 m²). In fact, this threshold mainly deletes small polygons on roofs that contain other larger suitable areas, generally the south facing part of the roof.

A monthly analysis shows the demand and production variation throughout the year (Figure 8). In summer, the production is limited by the demand and in winter by the resource. On both territories, solar thermal production would represent half of the total heat demand for DHW.

The third scenario is performed only in Pâquis due to a lack of information on the buildings heat consumption for space heating in Veyrier. The roof areas dedicated to SH and DHW thermal collectors represent 41,126 m². Therefore, it implies a high reduction of the areas to be used for PV panels. Solar thermal potential for SH and DHW is estimated at 11,525 MWh. The productivity of 280 kWh/m² is relatively low compared to the productivity of thermal collectors only for DHW. The reason is the temporal non-adequacy between solar

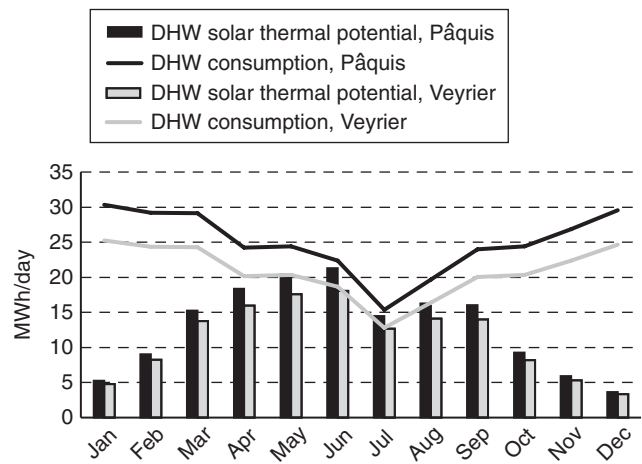


Figure 8: Monthly DHW consumption and DHW solar thermal potential in scenario 2.

resource and heat demand (Figure 9). Months with the highest potential are March, April and October. Only 13% of the annual heat demand for SH and DHW would be covered by solar production.

The PV potentials in the second and the third scenarios are lower than in the first scenario, some roof areas being used for thermal collectors. In the second scenario, this spatial competition implies a reduction of 18 and 9% of the PV potential in Pâquis and Veyrier, as compared to the first scenario. The decrease is more important in Pâquis due to the population density related to the built area, resulting in larger solar thermal collector areas.

With space heating applications, the PV potential reduction in comparison to the first scenario is more important and amounts to 74%. The next graphs summarize the results for the three scenarios (Figure 10).

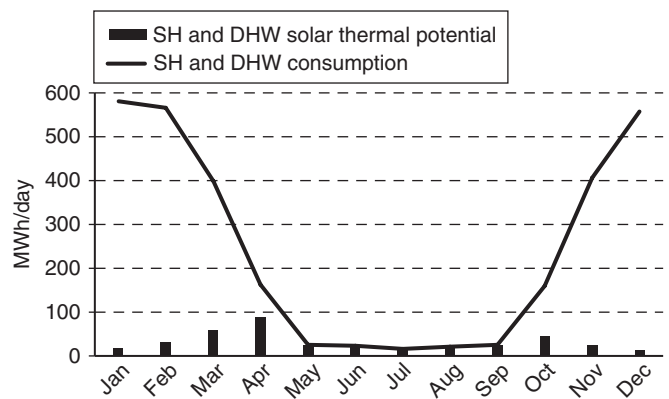


Figure 9: Monthly DHW&SH consumption and DHW&SH solar thermal potential in scenario 3 (only for Pâquis).

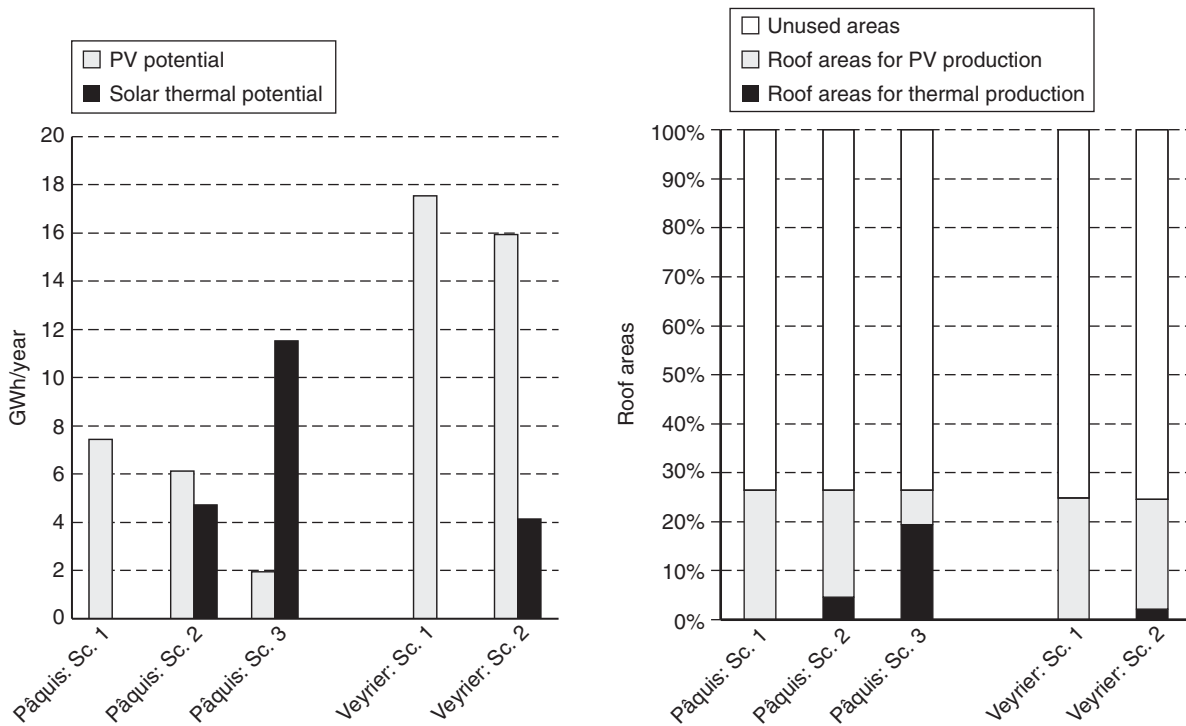


Figure 10: Solar potentials (left) and roof areas allocation (right) for each scenario.

Finally, we performed a sensitivity analysis on the sizing key for solar thermal collectors (expressed in $m^2/pers$ in scenario 2 and in m^2/MWh in scenario 3) in order to assess its influence on the respective thermal

and PV production (Figures 11-12). In these figures the “base case” (100%) corresponds to the recommended sizing keys (presented in section 2.3.2 and 2.3.3), which are up or down scaled for the sensitivity analysis.

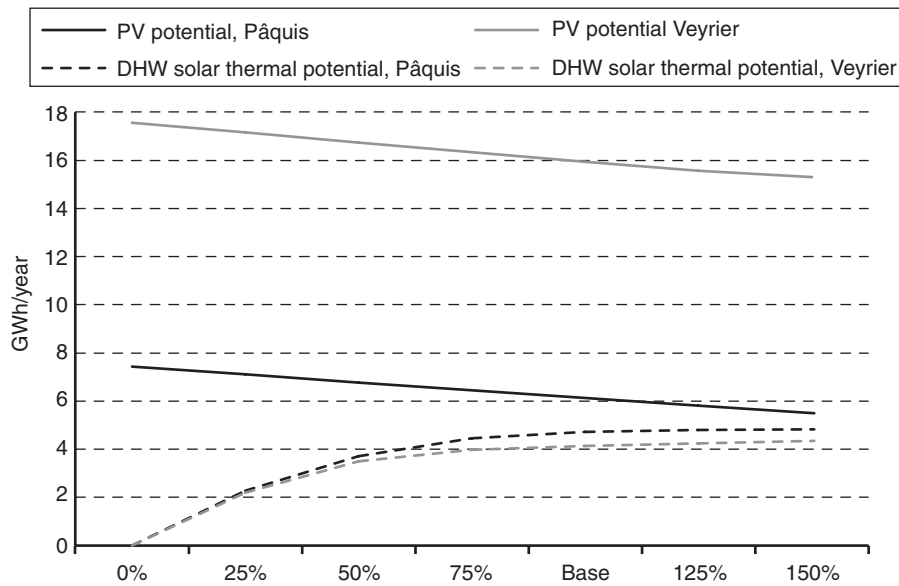


Figure 11: Influence of the DHW solar thermal collectors sizing on PV potential.

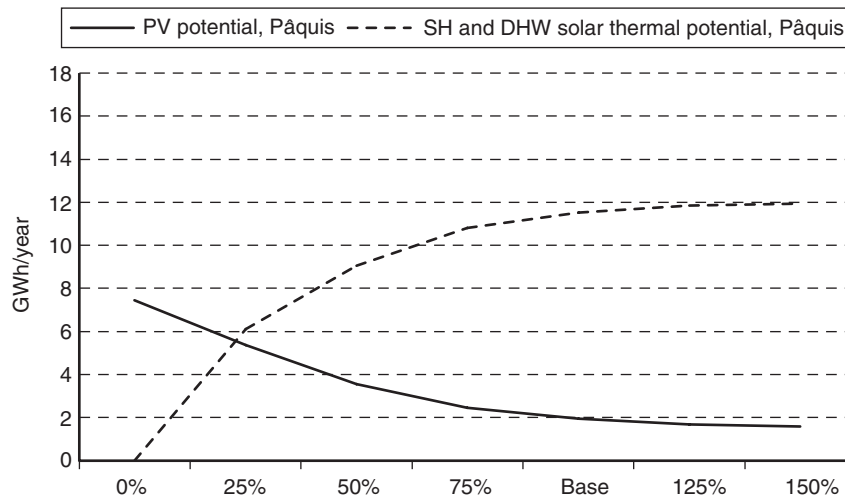


Figure 12: Influence of the SH and DHW solar thermal collectors sizing on PV potential (only for Pâquis).

Concerning solar collectors for DHW (Figure 11), up scaling of the sizing key by a factor 1.5 would hardly bring any additional thermal yield (+2.1% in Pâquis, +4.9% in Veyrier), while further reducing the PV production (−10.4% in Pâquis, −4% in Veyrier). In the case of combined DHW and SH production (Figure 12), up scaling of the sizing key doesn't either bring any additional thermal yield, but neither reduces the PV production. As a matter of fact, at least in the case of Pâquis, the recommended sizing rule usually turns out higher than the available roof area, so that up scaling of the rule is not effectively feasible (see section 2.3, adaptation of the sizing rule to the available roof area).

5. Discussion

The comparison between two territories with different characteristics demonstrates that urban morphology has an important impact on solar useful energy potentials. The main variables are buildings typology and population density. The results show that PV potential depends mostly on the suitable roof areas whereas solar thermal potential is more related to the demand. A comparison of different scenarios demonstrates that combining PV and solar thermal for DHW is relevant in both territories. Actually, the installation of properly sized solar thermal collectors doesn't decrease much the solar PV potential. However, a sensitivity analysis demonstrates that an oversizing of solar thermal installations implies a decrease of PV potential and is not really relevant from an energetic point of view. Solar thermal collectors for combined SH and DHW take more space and thus reduce

even more the PV potential. Hence, this solar application doesn't appear relevant without seasonal storage possibilities. Finally, a key issue behind the comparison of different scenarios is the comparison between thermal and electrical energy, taking into account that the latter is a more valuable and non-restrictive useful form of energy.

From a methodological point of view, application of the model to other locations would need a preliminary recalibration of the coefficients for the calculation of DHW and SH production (eq.3 and 5), by way of an appropriate numerical simulation campaign. As a first approximation, the input/output curves used in this study could however be used for locations which are characterized by similar climatic distributions within the months, as well as a similar radiation/temperature relation, which is typically the case for Central European climates. Considering PV, it may be necessary to adjust slightly the PV efficiency value which may depend on geographical location.

Because of the fact that heat and electricity are difficult to compare, the economic aspects of the different scenarios have not been assessed and compared. Furthermore, the variety of production costs observed (especially for solar thermal) and the fact that they are changing very rapidly from one year to another (especially for PV) make it difficult to realize a consistent comparison [33].

Finally, it should be noticed that within this study we assume a restriction of the solar thermal production by the demand, but not so for the PV production, which is injected in the grid. This

assumption is valid as long as the penetration rate of fluctuant renewable electricity production remains relatively low, beyond which it also becomes necessary to store or convert excess electricity, and/or to strengthen the grid. On the contrary, the limitation due to local building heat demand regarding solar thermal potential could be less problematic with the development of low temperature district heating. Excess heat production could be injected into such thermal networks and consumed by other consumers. The possibility to share large heat storage capacities could also facilitate the use of solar energy for space heating applications (seasonal storage).

6. Conclusion

This paper describes a complete method for estimating the solar energy potential at the level of an urban territory. In addition to determination of the solar resource on the building roofs, the model allows for evaluation of PV potential as well as solar thermal production potentials for DHW or combined DHW/SH. The method, which was developed and tested for the case of Geneva, could be transposed to another region, provided: (i) that a minimum dataset is available, in particular a digital surface model for determination of the solar resource, as well as GIS data concerning the number of inhabitants and/or the annual building thermal demand for DHW and SH application; (ii) that the input/output models for solar thermal application be adapted (for example by way of region specific numerical simulation on such systems).

The model was tested and analyzed for two different territories of Geneva (city center and rural suburban town). In the case of sole PV production (which mainly relates to the available and suitable roof areas), the average panel related productivity turns out to be similar in both territories (about 135 kWh/m²). Due to different population densities as related to the built area, the per capita production however differs: about 700 kWh/pers in the city center, respectively 1,870 kWh/pers in the rural suburban town. The installation of properly sized solar thermal collectors for DHW doesn't modify the solar PV potential very much (580 respectively 1'690 kWh/pers), while allowing for substantial thermal production (about 440 kWh/pers in both cases). On the contrary, thermal collectors for combined SH and DHW (which could only be computed for the city center) take up much more space and drastically reduce the PV potential (180 kWh/pers). Although the thermal

potential more than doubles (1,080 kWh/pers), the overall result is less appealing than for the previous case, the energetic and economic value of heat being less than that of electricity.

Acknowledgements

We are grateful to Alain Dubois and Pierre Lacroix from University of Geneva for their advice in GIS and to Pierre Ineichen from University of Geneva for handing out of the solar irradiation data and advice for calibration of the solar irradiation model. This research has partially been financed by CTI within the SCCER FEED&D (CTI.2014.0119) and by the Industrial Services of Geneva (SIG).

References

- [1] Sorensen B, GIS management of solar resource data. *Solar Energy Materials and Solar Cells* 67 (1-4) (2001) pages 503-509. <http://www.sciencedirect.com/science/article/pii/S0927024800003196>
- [2] Suri M, Huld TA, Dunlop ED, Ossenbrink. Potential of solar electricity generation in the European Union member states and candidate countries. *Solar Energy* 81 (10) (2007) pages 1295-1305. <http://www.sciencedirect.com/science/article/pii/S0038092X07000229>
- [3] Oloo F, Olang L, Strobl J. Spatial modelling of solar energy potential in Kenya. *International journal of Sustainable Energy Planning and Management* (2015).
- [4] Wiginton L, Ngueyen H, Pearce J. Quantifying rooftop solar photovoltaic potential for regional renewable energy policy. *Computers, Environment and Urban Systems* 34 (4) (2010) pages 345-357. <http://www.sciencedirect.com/science/article/pii/S0198971510000025>
- [5] Izquierdo S, Rodrigues M, Norberto F. A method for estimating the geographical distribution of the available roof surface area for large-scale photovoltaic energy-potential evaluations. *Solar Energy* 82 (10) (2008) pages 929-939. <http://www.sciencedirect.com/science/article/pii/S0038092X08000625>
- [6] NET, Nowak Energie & Technologie AG. Le potentiel solaire dans le canton de Genève : analyse et évaluation du potentiel solaire – photovoltaïque et thermique – dans le parc immobilier public du canton de Genève. 2004 [Technical report]. http://www.netenergy.ch/pdf/potentiel_solaire_geneve.pdf
- [7] Brito MC, Gomes N, Santos T, Tenedorio JA. Photovoltaic potential in a lisbon suburb using LiDAR data. Elsevier editorial system for solar energy. (2011). http://www.academia.edu/1179172/Photovoltaic_potential_in_a_Lisbon_suburb_using_LiDAR_data

- [8] Carneiro C, Morello E, Desthieux G. Assessment of solar irradiance on the urban fabric for the production of renewable energy using LIDAR data and image processing techniques. *Lecture Notes in Geoinformation and cartography*, (2009) pages 83–112.
- [9] Choi Y, Rayl J, Tammineedi C, Brownson J. PV analyst: coupling ArcGIS with TRNSYS to assess distributed photovoltaic potential in urban areas. *Solar Energy* 85 (11) (2011) pages 2924–2939. <http://www.sciencedirect.com/science/article/pii/S0038092X11003070>
- [10] Hofierka J, Kanuk J. Assessment of photovoltaic potential in urban areas using open-source solar radiation tools. *Renewable Energy* 34 (10) (2009) pages 2206–2214. <http://www.sciencedirect.com/science/article/pii/S0960148109000949>
- [11] Redweik P, Catita C, Brito M. Solar energy potential on roofs and facades in an urban landscape. *Solar Energy* 97 (2013) pages 332–341. <http://www.sciencedirect.com/science/article/pii/S0038092X13003460>
- [12] Dean J, Kandt A, Burman K, Lisell L, Helm C. Analysis of web-based solar photovoltaic mapping tools. *Proceedings of the 3rd International Conference on Energy sustainability*, San Francisco. 2009. <http://regisindia.com/wp-content/uploads/2013/10/Analysis-of-Web-based-Solar-Photovoltaic-Mapping-Tools.pdf>
- [13] Gadsden S, Rylatt M, Lomas K, Robinson D. Predicting the urban solar fraction: a methodology for energy advisers and planners based on GIS. *Energy and Buildings* 35 (1) (2003) pages 37–48. <http://www.sciencedirect.com/science/article/pii/S0378778802000786>
- [14] Rylatt M, Gadsden S, Lomas K. Using GIS to estimate the replacement potential of solar energy for urban dwellings. *Environment and Planning B-Planning and Design* 30 (1) (2003) pages 51–68. <http://www.envplan.com/abstract.cgi?id=b12931>
- [15] Ampatzi E, Knight I, Wiltshire R. The potential contribution of solar thermal collection and storage systems to meeting the energy requirements of North European Housing. *Solar Energy* 91 (2013) pages 402–421. <http://www.sciencedirect.com/science/article/pii/S0038092X12003325>
- [16] SITG, Système d'information du territoire à Genève. 2012. Geodata. <http://ge.ch/sitg/>
- [17] Ineichen P. Solar radiation resource in Geneva, measurements, modeling, data quality control, format and accessibility. University of Geneva, 2013 [Technical report]. <http://archive-ouverte.unige.ch/unige:29599>
- [18] Fu P, Rich PM. Design and implementation of the Solar Analyst: an ArcView extension for modeling solar radiation at landscape scales. *Proc. IX Annual ESRI User Conference*. 1999. <http://proceedings.esri.com/library/userconf/proc99/proceed/papers/pap867/p867.htm>
- [19] ESRI. ArcGIS Spatial analyst – Solar analysis. 2012. <http://www.esri.com/software/arcgis/extensions/spatialanalyst/key-features/solar>
- [20] Kucuksari S, Khaleghi A, Hamidi M, Zhang Y, Szidarovszky F, Bayraksan G, Son YJ. An Integrated GIS, optimization and simulation framework for optimal PV size and location in campus area environments. *Applied Energy* 113 (2014) pages 1601–1613 <http://www.sciencedirect.com/science/article/pii/S0306261913007381>
- [21] Chaves A, Bahill AT. Pilot study uses DEM derived from LiDAR. *ArcUser Magazine for the Esri Software Users* (2010) pages 24–27. <http://www.esri.com/news/arcuser/1010/files/solarsiting.pdf>
- [22] Scartezzini JL. Toward zero energy buildings, from nano to urban scale. *International conference ENERGY in BUILDINGS. ASHRAE*. Athens, 2013. <http://www.ashrae.gr/perch/resources/einb2013/presentationscartezzini.pdf>
- [23] Compagnon R. Solar and daylight availability in urban areas. *Solar and daylight availability in the urban fabric. Energy and Buildings* 36 (2004) pages 321–328.
- [24] Ludwig D, Lanig S, Klärle M. Sun-area towards location-based analysis for solar panels by high resolution remote sensors (LiDAR). *Proceedings of International Cartography Conference*, Santiago de Chile. 2009.
- [25] Zraggen JM. Bâtiments résidentiels locatifs à haute performance énergétique : objectifs et réalités. University of Geneva, 2010 [PhD Thesis]. <http://archive-ouverte.unige.ch/unige:13093>
- [26] OFEN, Office fédéral de l'énergie. Dimensionnement d'installations à capteurs solaires. 2000. <http://www.suisse-energie.ch>
- [27] Lachal B. Etude sur le subventionnement des capteurs solaires thermiques à Genève. University of Geneva, 2002 [Technical report].
- [28] Guisan O, Lachal B, Mermoud A. Universal daily input/output diagrams for thermal solar collection subsystem: part 1. *Solar Energy* 8 (1990) pages 121–135. <http://www.tandfonline.com/doi/abs/10.1080/01425919008909715#.VMZIM9KG8pk>
- [29] Guisan O, Lachal B, Mermoud A. Universal daily input/output diagrams for thermal solar collection subsystem: part 2. *Solar Energy* 8 (1990) pages 203–219. <http://www.tandfonline.com/doi/abs/10.1080/01425919008909723?journalCode=gsol19#.VMZIBtKG8pk>
- [30] Lachal B. Enercad, calcul de la production de chaleur de capteurs solaires sur une base mensuelle. University of Geneva, 2000 [Technical report].

- [31] SIA, Swiss society of engineers and architects. Energy performance certificate of buildings. 2009. <http://www.sia.ch>
- [32] Quiquerez L, Cabrera D, Lachal B, Hollmuller P. Température de distribution de chauffage du parc immobilier genevois. Etat des lieux et évaluation du potentiel d'optimisation à partir de mesures in situ sur un échantillon de bâtiments. University of Geneva, 2013 [Technical report]. <http://archive-ouverte.unige.ch/unige:27989>
- [33] Conseil fédéral suisse. Comparaison de technologie : chaleur solaire et photovoltaïque. 2015. <http://www.news.admin.ch/NSBSubscriber/message/attachments/38425.pdf>